Engineering Structures 122 (2016) 83–92

Contents lists available at ScienceDirect

Engineering Structures

journal homepage: www.elsevier.com/locate/engstruct

Seismic evaluation of modular steel buildings

Amirahmad Fathieh *, Oya Mercan

Department of Civil Engineering, University of Toronto, Toronto, ON M5S 1A4, Canada

ARTICLE INFO

Article history:
Received 3 December 2014
Revised 25 April 2016
Accepted 26 April 2016
Available online 25 May 2016

Keywords:
Modular steel buildings
Three dimensional Incremental Dynamic Analysis (IDA)
Push-over analysis
Concentrically steel braced frame
Seismic design
Diaphragm interaction
Collapse capacity
Lateral stiffness
Nonlinear dynamic analysis
Inter-story drift

ABSTRACT

Modular steel construction is a relatively new construction technique that considerably reduces the time spent on the construction site. However, due to the detailing and assembly requirements of multi-story modular steel buildings (MSBs), these systems are prone to undesirable failure mechanisms during large earthquakes. In this paper a 4-story MSB is designed considering realistic constraints posed during the modular construction. Using a detailed model in OpenSees an assessment of the seismic demand and capacity of this MSB is provided by performing nonlinear static pushover and incremental dynamic analyses (IDA) in two and three dimensions. Diaphragm interactions, relative displacements and rotations between modules, the force transfer through horizontal connections, column discontinuity coupled with possible high inelasticity concentration in vertical connections are some other important aspects that are specifically considered. The results that are summarized with relevant conclusions provide a better insight to the dynamic behavior of multi-story MSBs.

1. Introduction

The modular method of construction is a fast evolving technique, and it is an alternative to traditional on-site construction. A modular building contains multiple prefabricated units called "modules". Modules are prefabricated in a remote facility, transported to a site with a ready foundation and assembled on-site to produce permanent residential or commercial buildings. Each unit is often fully equipped with facilities such as plumbing, flooring, and lighting at the factory. The applications of modular construction include apartments, schools, hotels, hospitals, offices, military and any other buildings where cellular and repetitive units are preferred. Improved accuracy and quality, fast on-site installation, and lower waste material are the main motivations for owners to prefer modular construction. Although modular steel building systems differ significantly from traditional on-site buildings in terms of their behavior, detailing requirements and method of construction, limited studies have been conducted to evaluate the seismic behavior of these structures [1,2].

To provide insight to the modular steel building (MSB) structure's capacity and understand the system behavior from a global perspective, a comprehensive study has been conducted on a typical MSB structure designed considering realistic constraints imposed by modular construction. In the first step, the 4-story MSB structure has been modeled in [3] OpenSees in two (2D) and three dimensions (3D). Then, to assess the global capacity of the structure and to have an understanding of its safety in comparison with traditional steel buildings, numerical simulations using incremental dynamic analysis (IDA) have been carried out. The effects of considering horizontal and vertical connections and their contribution in the overall structural response have also been evaluated. Using the 3D model, the diaphragm interactions in the MSBs and the interaction between the modules, the axial and shear forces in the connections that occur due to the relative displacements and rotations between the modules have also been captured [4]. This is followed by nonlinear static pushover analysis of the structure to investigate the relationship between the global result of the IDA and static pushover. As a widely adopted method in engineering practice, static pushover is used to determine the ultimate lateral load resistance of the structure. The results obtained from pushover analysis can be compared to the results from IDA. In this paper the results from all analyses are summarized with relevant conclusions.

* Corresponding author. Tel.: +1 647 981 6479.
E-mail addresses: amir.fathieh@alum.utoronto.ca (A. Fathieh), oya.mercan@utoronto.ca (O. Mercan).

http://dx.doi.org/10.1016/j.engstruct.2016.04.054
0141-0296/

2. Design and modeling of a typical MSB

Due to the complexity of the structural interaction within a group of modular units a detailed model of the entire structure is required to provide more realistic and reliable results. In a MSB structure, units are tied at their corners so that they act together to transfer lateral loads. Horizontal forces may be transferred by tension and compression forces in the ties at the corner of the modules and through the horizontal connections implemented in between them. By utilizing the diaphragm action of the floor and ceiling of each module, these forces are transferred to the corner connections. Because of potential articulation through the bolts and connecting plates at the connections, relative displacements and rotations may occur in between the modules (both horizontally and vertically).

In structural analysis, two-dimensional and three-dimensional computer models can be used. When P–Δ effects are to be considered in the analysis, two-dimensional models must include the tributary gravity carrying system of the Seismic Force Resisting System (SFRS) elements. The gravity system can be explicitly modeled or represented by means of leaning P–Δ columns. However, considering the advanced modeling and analysis tools that are now available, it is generally preferable to use a three-dimensional model of the entire structure for seismic analysis, even if independent analyses are performed along each orthogonal direction [5]. Analyzing the 3D model of a structure has several advantages. For instance, it provides a three-dimensional representation of the structure stiffness (for any analysis), mass (for dynamic analysis), and strength (for nonlinear analysis) properties. Therefore, the torsional response of the structure is explicitly included in the analysis and the distribution of the seismic effects in the various components of the SFRS is directly obtained from the analysis.

To conduct a nonlinear analysis, essential characteristics of all elements such as load-deformation or moment curvature characteristics in the model are required. To achieve the most reliable and realistic results different elements and materials have been tested both separately and in interaction with other components in the numerical analyses. In this study, a four story MSB structure is designed, introduced, and evaluated in both 2D and 3D with IDA and pushover analysis methods.

2.1. Model description

Considering earthquake forces and gravity loading, members of the 4-story braced MSB are seismically designed based on the National Building Code of Canada [6] (NBCC 2010). The seismic force resisting system of the 4-story braced MSB is shown in Fig. 1. There are 12 modules at each level dimensioned 3.5 m by 4 m with a height of 3.5 m. Since each module has its own columns installed off-site (i.e., at a remote factory), there may be more than one column at each axis of the building when the units are installed next to one another on-site (see Fig. 1a). The column sections comply with the maximum practical size of the columns which is 150 × 150 × 12.5 mm and are installed with a horizontal center to center distance of 0.35 m. Table 1 lists the frame sections for the columns, beams and braces for the MSB structure. Square Hollow Structural Sections (HSS), which are commonly used in MSB structures, are chosen for all the columns and braces and wide flange sections (W shape) are used for the ceiling and floor beams. The design load of floor materials is based on a typical floor system where the weights of the concrete floor, insulation, a steel deck, self-weight of the frame members, and an all-around metal curtain wall have been considered. Superimposed dead loads of 0.75, 0.32, and 0.7 kN/m^2 are introduced to account for additional loads on floor, roof, and ceiling respectively. The design live loads of 1.9 kN/m^2 for the rooms, 4.8 kN/m^2 for the corridors, and a snow load of 1.0 kN/m^2 are assumed in accordance with NBCC (2010) and the seismic loads are for the city of Vancouver, Canada. CISC Grade 350 W steel with a specified yield stress, F_y, of 350 MPa is assigned to all the structural members.

2.2. Vertical and horizontal connections

In a MSB structure, units are tied at their corners so that they act together to transfer lateral loads. In some cases, for corner supported modules, a gap between the floor and ceiling beams are allowed to facilitate bolting or welding and let the mechanical and electrical facilities run along the building. Therefore, in this model a 0.15 m clear space between the floor and ceiling beam is provided. The modules are connected to each other in the vertical direction through the vertical connections of the columns (Fig. 2a).

Table 1
Member sections from the seismic design.

4-Story MSB			
Story #	Columns	Braces	Beams
4	HSS 76 × 76 × 5	HSS 51 × 51 × 5	W 100 × 19
3	HSS 102 × 102 × 6	HSS 51 × 51 × 5	W 100 × 19
2	HSS 102 × 102 × 6	HSS 76 × 76 × 5	W 100 × 19
1	HSS 127 × 127 × 5	HSS 76 × 76 × 5	W 100 × 19

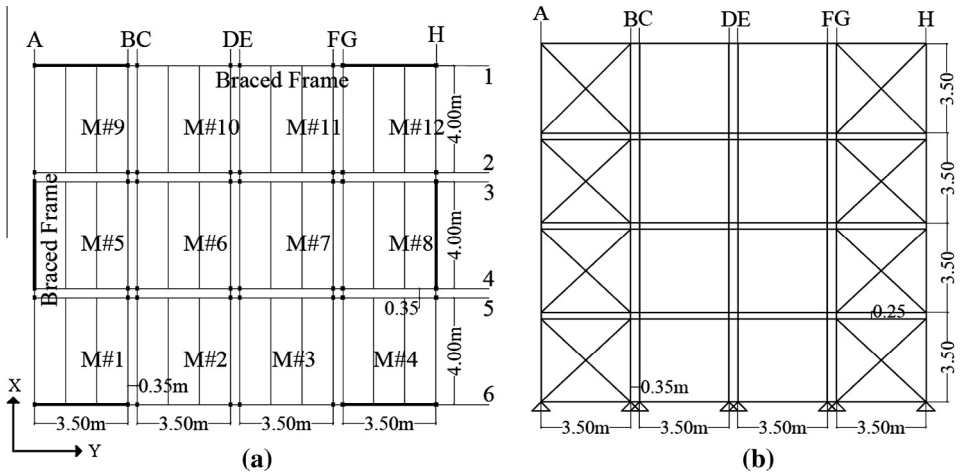

Fig. 1. 4-story MSB braced frame (a) floor plan and (b) elevation of frame 1 or 6.

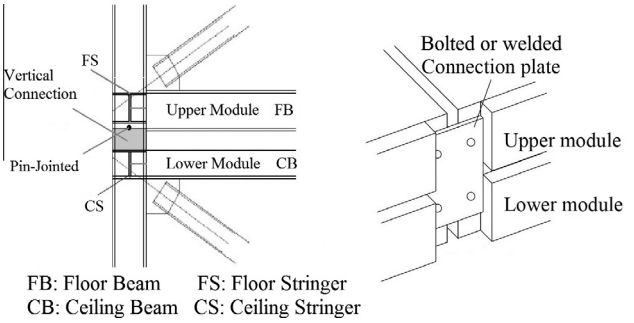

Fig. 2. (a) Vertical connection and (b) horizontal connection between the modules.

Similar to the analytical and experimental work by Annan et al. [7] (2009), for beam and columns rigid connections are used. Elastic beam–column elements are defined as rigid blocks at the end of the beams and columns. The rigid portions of the connection start at the beam–columns intersection node and continue up to half the section's total depth. To capture the independent rotations at the end of the columns caused by the partial field welding of the modules, a short column segment is located between the top flange of the lower ceiling beam and the bottom flange of the upper unit floor beam. This short column is an inelastic force beam–column element (OpenSees) with the same section properties as the lower column connected to it. A joint is introduced at the top end of each short column to simulate the independent rotation at the vertical connections (pinned). The horizontal connections of separately finished units are achieved by bolting steel plates or shop-welded clip angles (Fig. 2b) to the floors at the corners of the modules [8,9]. It is assumed that these connections are designed so that they remain elastic under the design earthquake. This is achieved by assigning an element with shear and bending strength of 1.3 times the adjacent beams at the intersection of the horizontal connections.

2.3. Beams and columns

In the OpenSees model, inelastic steel beam–column elements have been used to represent all the beams and columns of the MSB frame. These elements are ForceBeamColumn elements with two nonlinear definable sections at both ends of the section, with an elastic segment at the middle portion of each element. They act as nonlinear beam–column elements with distributed plastic hinges at both ends. The hinges are defined by assigning rotational springs at both ends of the element and localize the plasticity at the specific hinges (beamWithHinge), therefore the integration points (gauss points) will be limited to these regions [10].

2.4. Braces

Diagonal braces of the MSB frame experience global plastic mechanisms and are subjected to large cyclic deformations during strong earthquakes. The mechanism is achieved through the yielding of a brace in tension and the inelastic buckling of the brace in compression. The buckling and post-buckling of the brace forms three flexural plastic hinges. The tension-yielding brace deforms inelastically through axial inelastic deformation, and plastic rotations of the flexural plastic hinges occur in compression as the brace buckles. To model the braces and capture a realistic buckling behavior, the fiber-based model developed by Uriz and Mahin [11], has been used. To allow the formation of the three above-mentioned flexural plastic hinges, as can be seen in Fig. 3a, the brace is divided into different separated segments. The model can realistically represent the buckling behavior of the brace members and capture the inelastic behavior under repetitive axial tension and compression considering the significant degradation in compressive resistance of the braces after a few cycles of loading. The force–deformation plot of one of these elements subjected to a harmonic loading is shown in Fig. 3b.

Brace, beam, and column connections need to be designed carefully to carry forces that are induced by the yielding of the tension braces and buckling of the compression braces. This is more important in MSB systems where the redistribution of the forces may not be as reliable due to the partial welding of the vertical connections at the end of the columns and also to the high inelasticity concentration at the vertical connections caused by the eccentricity of the brace working points.

3. Incremental dynamic analysis of the MSB structure

Evaluation of the performance of a structure requires a method that monitors the structure behavior from linear elastic region to yielding and collapse stage. For multi-degree of freedom (MDOF) structures the dynamic interaction of the higher modes can make it hard to predict the post yield behavior. Incremental Dynamic Analysis (IDA) is a widely used approach to evaluate the performance of structures. In this method, a set of ground motion records are chosen, each record is scaled into multiple intensity levels to cover the whole range of structural response. IDA curves consist of a set of scaled ground motion records known as Intensity Measure (IM) and a series of the structural response known as Demand

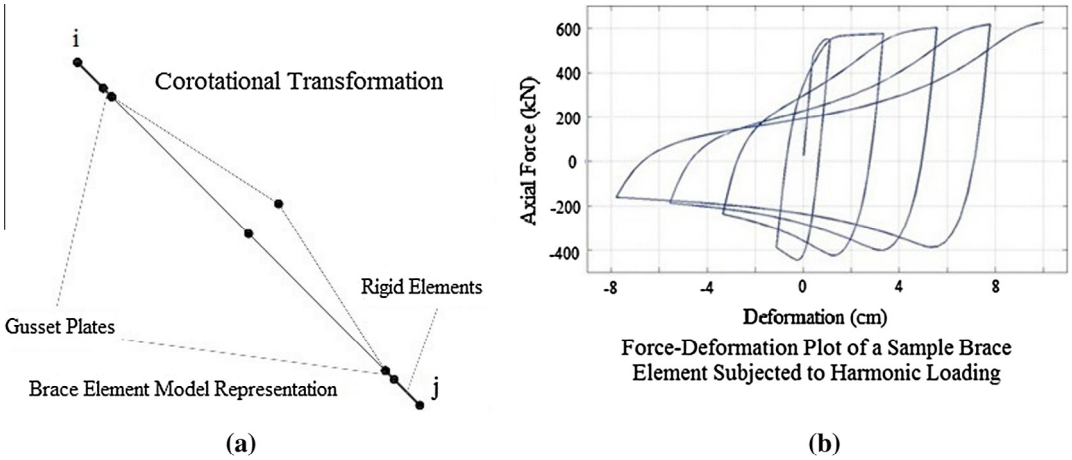

Fig. 3. (a) Brace finite element model and (b) force versus displacement relationship for a sample brace element.

Parameter (DP). Each DP versus IM produces a single point on the IDA plot. As a result, an IDA curve is generated from a series of IMs and DPs in a way that the curve is produced from different intensity values of a specific ground motion and their corresponding demand parameters. Since the response obtained from a single ground motion may not provide sufficient confidence of the dynamic behavior of the structure, a group of ground motion records needs to be considered. In this study the suite of 20 ground motions selected by Vamvatsikos and Cornell [12], was used (Table 2). The seismic inelastic demand of the structure is determined using the Incremental Dynamic Analysis (IDA) procedure. The spectral acceleration at 5% damping, Sa(T1, 5%), is used as initial Intensity Measure (IM). A simple stepping algorithm, with an initial IM value of 0.005 g and constant steps of 0.05 g, is employed to scale the ground motion records. This is described in detail by Vamvatsikos and Cornell [13].

Since failure of braces is more evident at larger inter-story drifts, it can represent both the local and global collapse and consequently, can be used as a reliable Damage Measure (DM). As a primary DM parameter, maximum inter-story drift is often used in both vulnerability assessment of moment resisting frames and characterizing global dynamic response of ductile concentrically braced frame structures.

The average first and second mode periods of the 3D 4-story MSB are 0.7 and 0.54 s and for the 2D building is 0.6 and 0.17 s. The fundamental lateral period (T_a) obtained from the NBCC code is 0.35 s. The spectral acceleration, Sa(T), corresponding to the fundamental period of the building is computed as 0.8 g. The maximum inter-story drift ratio, θ_{max}, and peak roof drift ratio, θ_{roof}, were selected as global demand parameters, DM, to evaluate the structural response. These DMs are plotted against corresponding Sa(T1, 5%) of the scaled ground motion records to obtain the IDA curves. Figs. 4 and 5 show the IDA curves for the 2D and 3D MSB in Z direction.

To summarize the large amount of data produced by IDAs, a statistical assessment of the demand is required. The data sets obtained under the suite of ground motions for the 2D and 3D models are compressed into probabilistic distribution of a DM given an IM by defining the 16%, 50%, and 84% fractile IDA curves (Figs. 6 and 7) [14].

As a representative of seismic demand parameter of the building, the fractile IDA curves may be used to evaluate the performance of the structure by comparing the calculated demands with allowable drift demands at any given IM and probability level. Based on the fractile curves it can be observed that given the design spectral acceleration of the site, the design ground motion

Table 2
Earthquake ground motion records selected from PEER Strong Ground Motion Database.

No.	Event	Year	Record station	ϕ^a	M^b	R^c (km)	PGA (g)
1	Imperial Valley	1979	Plaster City	45	6.5	31.7	0.042
2	Imperial Valley	1979	Plaster City	135	6.5	31.7	0.057
3	Imperial Valley	1979	Westmoreland Fire Sta.	90	6.5	15.1	0.074
4	Imperial Valley	1979	Westmoreland Fire Sta.	180	6.5	15.1	0.110
5	Imperial Valley	1979	El Centro Array # 13	140	6.5	21.9	0.117
6	Imperial Valley	1979	El Centro Array # 13	230	6.5	21.9	0.130
7	Imperial Valley	1979	Chihuahua	282	6.5	28.7	0.254
8	Imperial Valley	1979	Cucapah	85	6.9	23.6	0.309
9	Loma Prieta	1989	Agnews State Hospital	90	6.9	28.2	0.159
10	Loma Prieta	1989	Coyote Lake Dam	285	6.5	22.3	0.179
11	Loma Prieta	1989	Sunnyvale Colton Ave	270	6.9	28.8	0.207
12	Loma Prieta	1989	Sunnyvale Colton Ave	360	6.9	28.8	0.209
13	Loma Prieta	1989	Anderson Dam Down S.	270	6.9	21.4	0.244
14	Loma Prieta	1989	Hollister Diff. Array	165	6.9	25.8	0.269
15	Loma Prieta	1989	Hollister Diff. Array	255	6.9	25.8	0.279
16	Loma Prieta	1989	WAHO	0	6.9	16.9	0.370
17	Loma Prieta	1989	Hollister South & Pine	0	6.9	28.8	0.371
18	Loma Prieta	1989	WAHO	90	6.9	16.9	0.638
19	Superstition H.	1987	Wildlife Liquefaction A.	90	6.7	24.4	0.180
20	Superstition H.	1987	Wildlife Liquefaction A.	360	6.7	24.4	0.200

[a] Component.
[b] Moment magnitude.
[c] Closest distance to fault rupture.

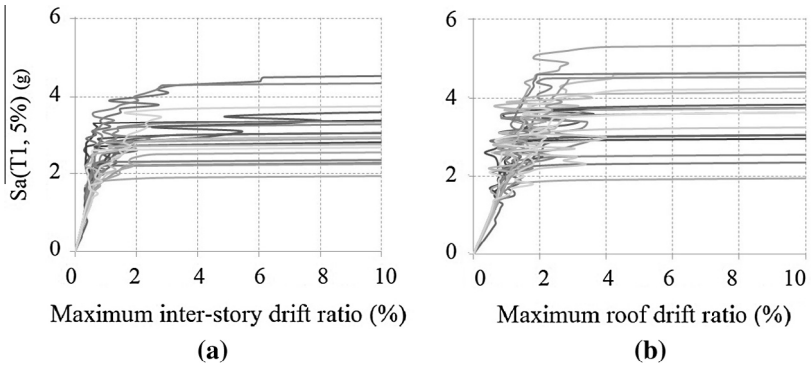

Fig. 4. IDA curves of "First Mode" spectral acceleration, Sa(T1, 5%), plotted against (a) maximum inter-story drift ratio, θ_{max}, (b) peak roof drift ratio, θ_{roof}, for the two-dimensional 4-story MSB-braced frame.

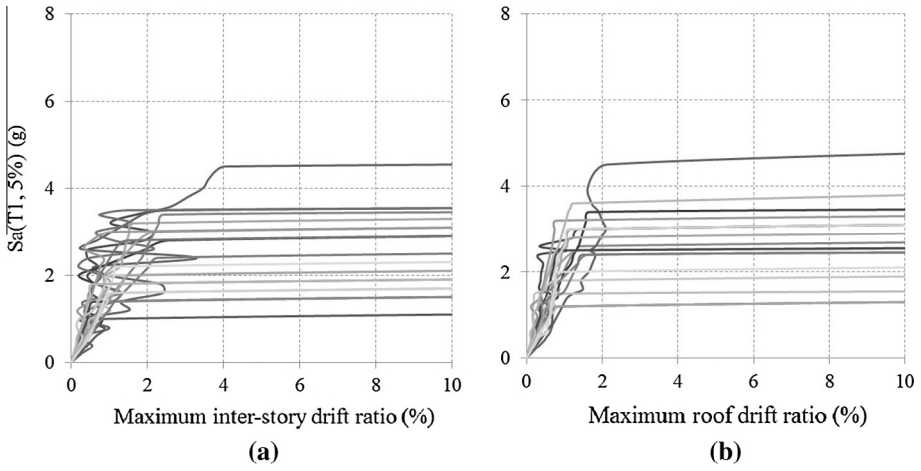

Fig. 5. IDA curves of "First Mode" spectral acceleration, Sa(T1, 5%), plotted against (a) maximum inter-story drift ratio, θ_{max}, (b) peak roof drift ratio, θ_{roof}, for the three-dimensional 4-story MSB structure in *Z* direction.

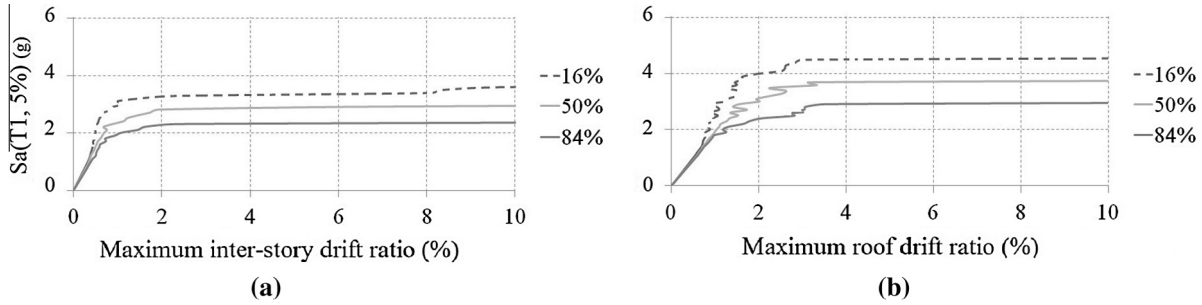

Fig. 6. Summary of IDA curves of the two-dimensional 4-story MSB frame into 16th, 50th, and 84th fractiles with (a) maximum inter-story drift ratio and (b) peak roof drift ratio.

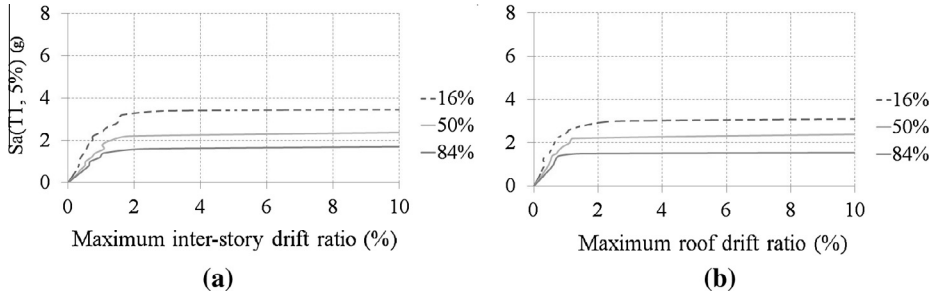

Fig. 7. Summary of IDA curves of the three-dimensional 4-story MSB structure (*Z* direction) into 16th, 50th, and 84th fractiles with (a) maximum inter-story drift ratio and (b) peak roof drift ratio.

intensity level of Sa(T1, 5%), at 2% in 50 year probability is 0.8 g. Accordingly, the calculated fractiles for the 3D model show that for the design level intensity, 50% of the records would produce $\theta_{max} < 0.52\%$; and for the 2D model 50% of the records would produce $\theta_{max} < 0.31\%$. In NBCC (2010) the largest inter-story deflection at any level which is based on median 2% in 50-year seismic hazard level should be limited to 0.01 h_s for post-disaster buildings, 0.02 h_s for high importance category buildings, and 0.025 h_s for all other buildings. Hence, it can be inferred that the median ground motions calculated for the MSB structure provides satisfactory performance in all of the above building categories. Table 3 summarizes the 16%, 50%, and 84% fractile values in terms of DM and IM for Immediate Occupancy (IO), Collapse Prevention (CP), and

Table 3
Summarized capacities for each limit-state for the 2D and 3D MSB models in *Z* direction.

	Sa(T1, 5%) (g)			θ_{max} (%)		
	$IM^c_{16\%}$	$IM^c_{50\%}$	$IM^c_{84\%}$	$DM^c_{16\%}$	$DM^c_{50\%}$	$DM^c_{84\%}$
2D Model						
IO	2.2	2.8	3.2	2	2	2
CP	2.4	2.9	3.7	10	10	10
GI	2.5	3.1	3.9	$+\infty$	$+\infty$	$+\infty$
3D Model						
IO	1.5	2.2	3.2	2	2	2
CP	1.8	2.4	3.4	10	10	10
GI	1.9	2.7	3.6	$+\infty$	$+\infty$	$+\infty$

Global Instability (GI) limit-states, for the 4-stories MSB-braced structure.

4. Inter-story drift of the modules

The inter-story drifts in the IDA and fractile plots provided above were obtained from the displacements of two consecutive floor beams in modular units. Although the influence of ceiling beams between these floors was included in the model, the extent of their contribution to the inter-story drift could not be shown in these plots (Figs. 4 and 5). In the model, the nodal masses were assigned both to the floor and ceiling nodes and during a ground motion event, the maximum inter-story drift angle may also be changed at the ceiling level within the same modular unit. This will alter the lateral deformation distribution along the building height. Figs. 8 and 9 show the inter-story drift distributions where the ceiling beams were individually considered. In these distributions the maximum drifts of the model are plotted in both *Z* and *X* (3D model) directions. These drifts are obtained from the ground motion recorded at EL Centro Array #13 (Imperial Valley earthquake) with the intensity levels of Sa(T1, 5%) = 0.3, 2.0, and 3.0 g. They are representative of the trend under other ground motions. It is observed that in the elastic range of response the height-wise distribution of the maximum inter-story drift varies from record to record for the MSB structure. It is also observed that the distribution of the maximum inter-story drifts along the height of the structure is not uniform but with an increasing ground motion intensity level larger drifts are concentrated at a specific story. In this study, in the inelastic range of response, the concentration of the inelasticity is mainly observed at the first story level of the structure. This trend is maintained as the intensity level of the ground motions increases. As it can be seen the figures, the contribution of the ceiling beams to the inter-story drift in this range is greater but still rather insignificant. For all other ground motions input applied, while exhibiting a similar pattern, the height-wise distributions of the drifts only vary in terms of amplitudes.

5. Horizontal connections and diaphragm action

Unlike regular steel buildings where a uniform slab is provided at every floor level, in MSB structures each module has its own

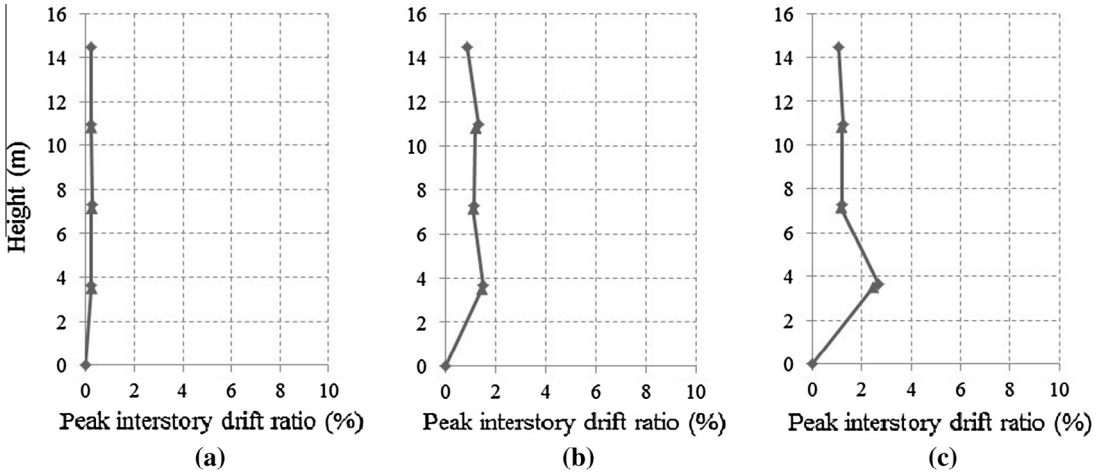

Fig. 8. Height-wise distribution of peak inter-story drift ratio for the 2D 4-story MSB (a) Sa(T1, 5%) = 0.3 g, (b) Sa(T1,5%) = 2.0 g, and (c) Sa(T1, 5%) = 3.0 g.

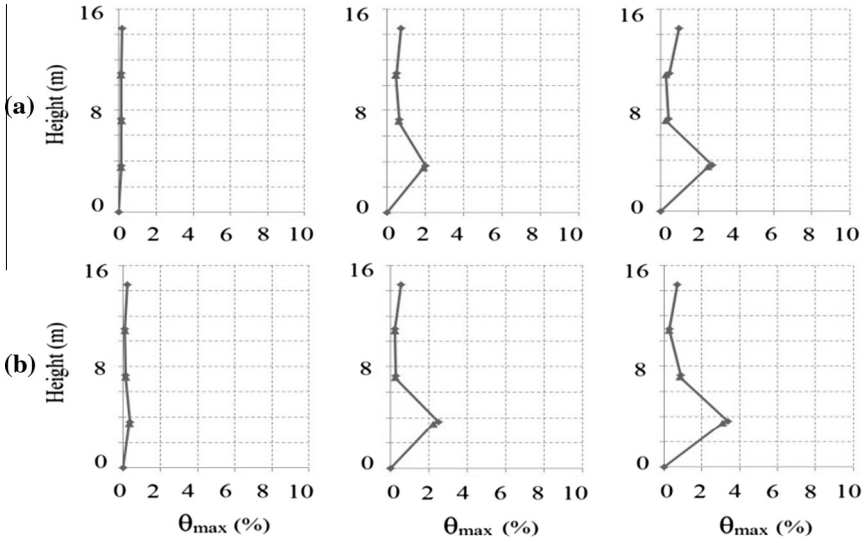

Fig. 9. Height-wise distribution of peak inter-story drift ratio for the 3D 4-story MSB at Sa(T1, 5%) = 0.3 g, 2.0 g and 3.0 g in (a) *Z* direction and (b) *X* direction.

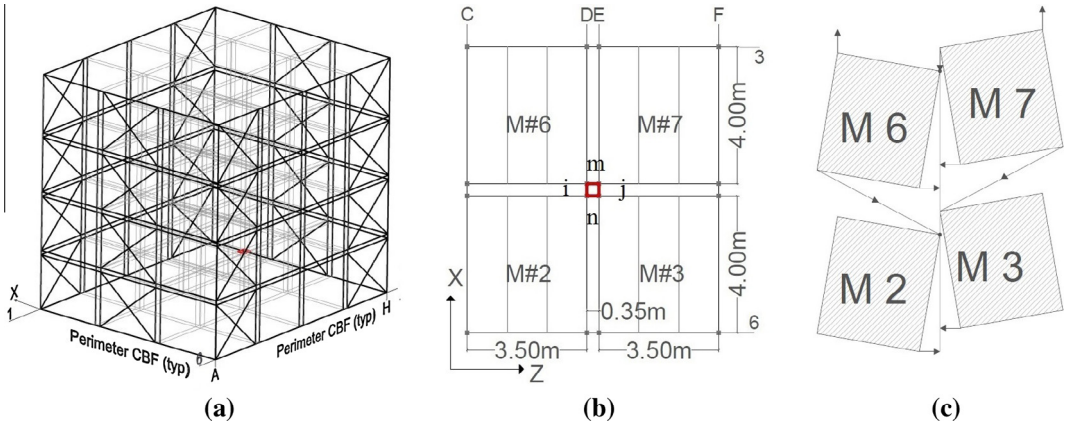

Fig. 10. MSB structure: (a) 3D view of the SFRS vertical elements; (b) plan view of four of the modules (diaphragms) that are connected through the horizontal connections located at the center of the modules; (c) relative displacement of modular units.

individual concrete slab. The connections between these slabs are provided through the horizontal connections (Fig. 10b). Hence, instead of having a single diaphragm, separated diaphragms (one for each module) should be considered at each story floor when modeling a MSB structure. This will also result in a more realistic representation of the braced frame lateral stiffness; and, thereby, provide better predictions of the building drifts and periods [5]. Moreover, by modeling diaphragms separately, the actual in-plane flexibility of the floors will be obtained more accurately, leading to more representative distributions of forces and deformations of the horizontal and vertical components.

The detailed 3D model enables the investigation of the internal forces in horizontal directions as well as the potential shear and bending actions in the connections. Apparently, in a 2D MSB model the axial forces (tension and compression) in the horizontal connections can be easily obtained; however, shear forces acting on the connections (out of plane forces which are perpendicular to the frame) cannot be captured. In the 3D model all the forces in two horizontal directions can be calculated together with their corresponding deformations and rotations. Figs. 11–13 examine these parameters (in global coordinates) for the three-dimensional model under the ground motion recorded at Hollister Diff. Array during the 1989 Loma Prieta. In these figures, time-history of internal forces, and comparative connection end displacements of selected horizontal corner connections which are located at the first floor ceiling level and floor level of the second floor are plotted (selected connections are highlighted in Fig. 10). It should be noted that in the selected inter-section, there are two floor beam and two ceiling beam connection elements in each direction and the total connection force is the sum of the two floor and two ceiling connection forces.

Figs. 11 and 13(a) show axial and shear forces in the floor and ceiling connections in (i–j) and (m–n) directions as well as the internal lateral moments for the floor connections. Table 4 shows the maximum values of corner connection elements internal forces (axial and shear forces in X and Z direction) as well as moments (about Y axis) at the first floor and for the ground motion recorded at Hollister Diff. Array during the 1989 Loma Prieta earthquake. Correspondingly, the horizontal displacements and rotations of the connections ends are recorded in Figs. 12 and 13(b). Maximum floor connection ends global displacement and rotations are also provided in Table 5. The difference between the two end displace-

Table 4
Maximum values of connection elements axial, shear, and moment forces in global coordinates.

Element	Connection	Axial (KN)	Shear (lateral) (KN)	Shear (vertical) (KN)	Moment (about Y axis) (KN m)
i–j	Floor	64.96	9.64	5.34	18.68
	Ceiling	55.84	8.66	3.58	19.24
m–n	Floor	66.98	12.9	3.0	27.8
	Ceiling	18.22	11.16	4.06	25.84

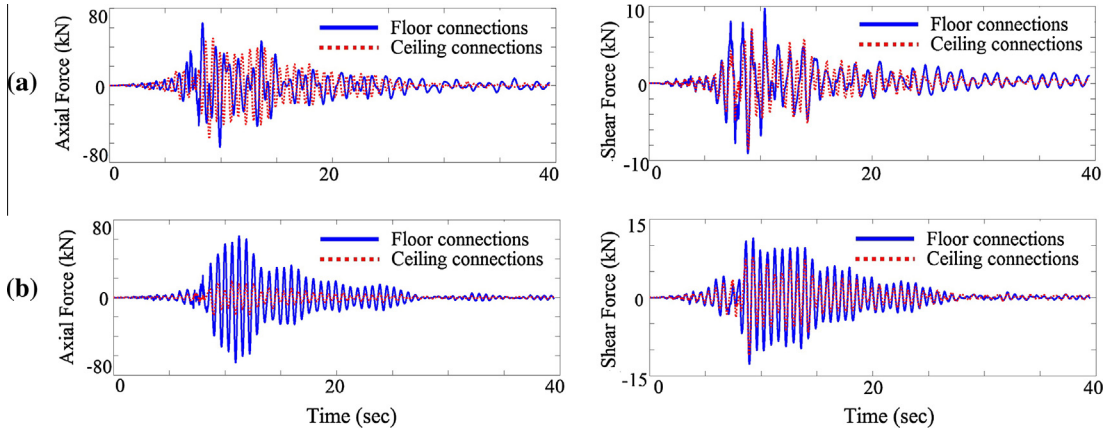

Fig. 11. Axial and shear forces in ceiling and floor connections in (a) [i–j] direction and (b) in [m–n] direction.

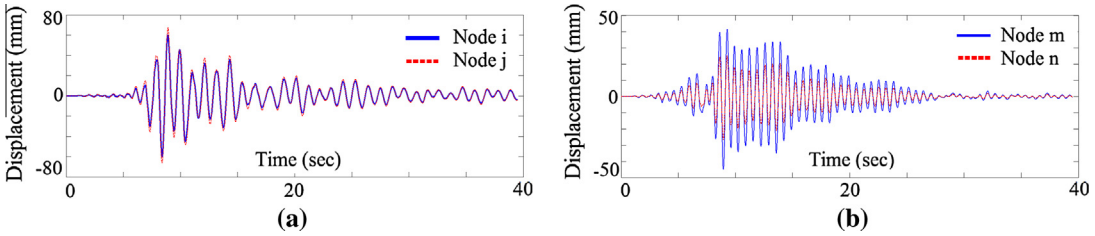

Fig. 12. End node displacements of connections; (a) displacement of end nodes of element (i–j) in X direction and (b) displacement of end nodes of element (m–n) in Z direction.

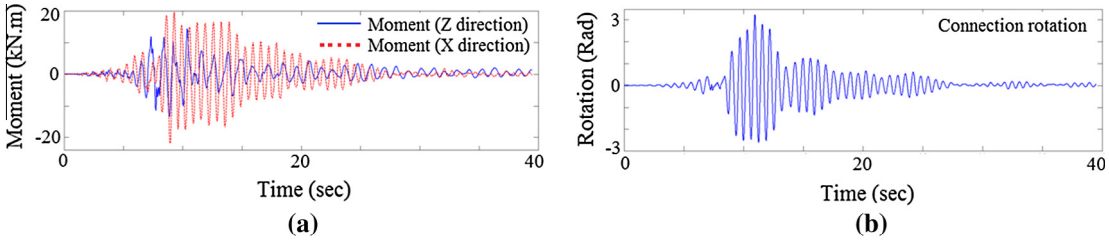

Fig. 13. (a) Internal lateral moment in the floor connections oriented in (i–j) and (m–n) directions and (b) connection (i–j) rotations.

Table 5
Maximum values of connection element nodal displacement and rotations.

Element node	Δ_X (m)	Δ_Y (m)	Δ_Z (m)	Θ_Y (Rad)
i	0.0604	0.0003	0.0449	0.0064
j	0.0673	0.005	0.0448	0.0064
n	0.0605	0.0002	0.0269	0.0062
m	0.0673	0.0003	0.0231	0.0062

ments is the relative displacement of the two sides of the connections (deformation) which is safely in the elastic range.

6. Comparison of the two-dimensional and three-dimensional MSBs

There are considerable differences between modular method of construction and conventional steel building construction. For example, non-SFRS beam to column connections in conventional braced-frame construction are usually achieved by shop or site welded/bolted clip angles or by connecting the webs of the beam and columns but not the flanges. The use of clip angles or partial welding in conventional construction results in the transfer of the forces at the ends of the beams through shear action, while allowing for partial rotation. Hence, the rotational stiffness of the connections of gravity frames and as a result their lateral resistances are usually ignored in structural response analysis of these structures. However, beam to column connections in MSB structures are achieved in a controlled factory environment by direct welding of the webs of the beams to the HSS columns.

The beam to column connection properties is simulated by rigid end connections attached to plastic hinges in order to not to restrict the development of plasticity in the columns provided in the MSB finite-element model, and the entire behavior of non-SFRS frames is taken into consideration.

Based on the results obtained from the IDA analysis of both the two-dimensional and three-dimensional MSB models introduced in this study, it can be concluded that the structural collapse capacity of the 3D model is "lower" than of the 2D model. This is because the 2D model fails to account for torsional effects and as a results overestimates the structural capacity against structural collapse.

Table 6
Comparison of collapse capacities obtained from 2D and 3D analysis (Z direction).

Model	$IM^{c}_{50\%}$: median capacity for CP (g)
2D modified MSB-braced frame	2.9
3D modified MSB-braced structure	2.4

Table 7
Maximum inter-story drift demand of the modified 4-Story MSB at the design intensity level (Z direction).

Model	$\theta_{max50\%}$: median inter-story drift ratio (%)
2D modified MSB-braced frame	0.31
3D modified MSB-braced structure	0.50

Given the design level ground motion intensity of Sa(T1, 5%) = 0.8 g, Table 6 compares the capacities of the two models for CP limit-state, and Table 7 shows the statistics of the maximum inter-story drift ratio demand at 2% probability of exceedance in 50 years.

7. Nonlinear pushover analyses in 2D and 3D

In this section, pushover analyses of the 2D and 3D 4 story MSB are carried out by incorporating the inelastic material behavior and effects of distributed plastic hinges at component ends. The finite element analysis is implemented using OpenSees. The gravity loads are applied initially in ten steps. This is followed by applying the distribution of lateral loads along the building height (at the center node of each diaphragm) of the structure. The predefined lateral load distribution pattern is based on NBCC (as a reference lateral load) and is applied incrementally; and the pushover analysis is displacement-controlled. The lateral forces are monotonically increased, until either a predetermined target displacement is reached or a non-convergence (i.e., collapse) happens. The inelastic static pushover analysis is a preferred approach for predicting the seismic force and deformation demands. It accounts

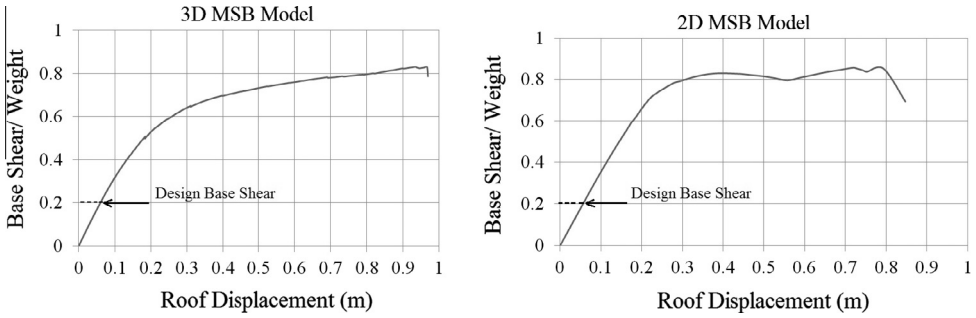

Fig. 14. Capacity (Pushover) curves of 2D and 3D MSB structures.

Table 8
Summary of pushover analysis for 2D and 3D MSB models.

Structural performance levels and damage – vertical elements				
Structural performance levels	Roof drift values (FEMA)	Corresponding roof displacement (m)	V/W[a] (2D)	V/W (3D)
IO (S-1)	0.7% transient or negligible permanent	0.098	0.348	0.311
LS (S-3)	2.5% transient or 1% permanent	0.35	0.82	0.67
CP (S-5)	5% transient or 5% permanent	0.7	0.85	0.78

[a] Base shear/weight of the structure.

for the redistribution of internal forces in both vertical and horizontal components when the structure is subjected to forces exceeding the elastic range of structural behavior. The analyses were performed until maximum roof displacement is equal to % 10 of the height of the building. While analyzing nonlinear structures convergence problems can be encountered. To ensure accuracy of the numerical solution, when using OpenSees as the simulation platform, a Solution Algorithm object can be defined. It determines a sequence of steps to be used to solve the nonlinear equations. In the event of non-convergence, several different algorithms can be queued to attempt to obtain a convergent solution. To be able to compare the results with those from IDA, the global capacity curve is obtained by plotting roof displacement versus base shear in Fig. 14. For the MSB considered in this study, the capacity curve represents the fundamental mode response of the structure since the first mode of vibration governing the response. For the evaluation of the performance of the building, the resulting capacity curves are also compared with provided Immediate Occupancy (IO), Life Safety (LS), and Collapse Prevention (CP) levels.

Similar to what was observed in IDA analyses, the distribution and order of the formation of the plastic hinges in braces depend on many factors. Analysis type, frame configuration, frame geometry, lateral load distribution, and the way that braces and other components are sized are some of these factors. As it was expected, in both 2D and 3D MSB structures under investigation in this study, with pushover analysis, the global ultimate strength is determined by structural mechanism and concentration of inelasticity in only one story. This is because the internal forces get distributed within a story, and when a mechanism forms, the alternative load paths are limited. In this case, the formation of mechanism through the yielding of a brace in tension and the inelastic buckling of the brace in compression leads to higher inter-story drift in the first story level and leading eventually to structural collapse. This was also observed in Annan et al.'s study (2009) on MSBs. The unique detailing of vertical connections appears to impose extra demand on the lower level columns causing the formation of plastic hinges at those locations. It should be pointed out that out of verticality of the columns may aggravate the second order effects, therefore the assembly of modules has to be very accurate and any lack of fit resulting excessive movements need to be avoided. The maximum value for out of verticality recommended is $\Delta <$ height/600, but <5 mm per story [8]. OpenSees includes material nonlinearity and adds the geometric stiffness matrix to element stiffness matrix to account for P–Δ effects.

According to [15] FEMA 356, the performance of a given structure is determined based the performance of both structural and nonstructural components. A specific performance level of a structure describes an approximate limit to structural and nonstructural damage that may be considered satisfactory for a given building under a ground motion. The three performance levels of IO (S-1), LS (S-3), and CP (S-5) are arranged based on decreasing performance of lateral and vertical Seismic Force Resisting Systems (SFRS) and are discrete damage states which are obtained from a continuous spectra of probable damage states, (Fig. 4). For braced steel frames, the structural performance levels and damages of vertical elements provided by FEMA 365 are gathered in Table 8. The response quantities from pushover analysis of both 2D and 3D structures at various performance levels with the corresponding base shear are also provided.

Considering the 3D model as an instance, it was observed that the maximum base shear ratio obtained at IO, LS, and CP are 0.31, 0.67, and 0.78, respectively. The relatively high values of the base shear ratios could be a result of the unique configuration of the MSB structures. As was mentioned before, the finished modules with 4 corner columns are installed on the site next to each other. Therefore there are multiple columns at middle and side axes of the building (two or four columns). Higher number of columns at the base would lead to more lateral resistance and consequently larger base shear at the base of the building.

As it can be seen in the table, similar to IDA analysis the structural capacity of the 3D model is found to be lower than that of the 2D model at different structural performance levels (IO, LS, and CP). This is because the 2D model fails to account for the torsional response, hence overestimating the structural capacity.

8. Conclusions

As a fast evolving and new method of construction, knowledge on the behavior of MSB structures is limited and there is no record of MSB performance under past earthquakes. In this study, as a

useful tool to quantify the seismic performance of structures, IDA was used to estimate the severity of the damage a MSB might suffer. An understanding of the distribution of inelasticity along the height of the MSB structure and the effect of ground motion intensities on maximum drift demand of the building were developed. The capacities at the Collapse Prevention level with their corresponding probabilities were estimated. Important findings from this study are summarized below:

1. Floor-to-floor inter-story drift can satisfactorily represent the inter-story drift demand and explicit consideration of the ceiling beam is not required. The predicted drift demands for the median ground motion records and at the design intensity level were satisfactory.
2. In the elastic range of response the distribution of the inter-story drift demand along the height of the structure varies from record to record. Due to the inelastic behavior of braces and the limited redistribution of the internal forces within the story levels the concentration of the inelasticity is found to be mainly in the first story level.
3. Modeling of separate diaphragms for each module instead of one rigid floor diaphragm at every floor level results in a realistic representation of the braced frame lateral stiffness, drift, and periods. At the design intensity level and for the selected number of modules, the relative displacements and rotations of the modules due to the horizontal forces were found to be insignificant.
4. Comparing the 2D and 3D models and according to both IDA and nonlinear pushover analysis, the structural capacity against incipient collapse of the 3D model was found to be lower than that of the 2D model. This is because the 2D model fails to account for the torsional response, hence overestimates the structural capacity.
5. Based on the results obtained from the nonlinear pushover analysis in both 2D and 3D models, it was observed that the maximum base shear that the structure can resist is relatively high in the MSB structures. This is due to considerably larger number of columns that bear the lateral shear in MSBs in comparison to regular traditional steel buildings.

In future studies the dynamic behavior of a series of mid to high-rise MSBs will be investigated. The results will be compared to the results obtained from equivalent traditional steel buildings to provide a stronger insight to the dynamic behavior of taller MSBs.

Acknowledgements

The financial support from NSERC Discovery 371627 and Engage EGP 445837 grants is gratefully acknowledged. The authors would like to thank Mr. Brent Roberts from Jerol Technologies for his input in modular building design. The opinions, findings and conclusions expressed here are those of the authors and do not necessarily reflect the views of the sponsors.

References

[1] Annan CD, Youssef MA, El Naggar MH. Seismic vulnerability assessment of modular steel buildings. J Earthquake Eng 2009;13(8):1065–88.
[2] Annan CD, Youssef MA, El Naggar MH. Seismic overstrength in braced frames of modular steel building. J Earthquake Eng 2009;13(1):1–21.
[3] Open System for Earthquake Engineering Simulation (OpenSees). <http://opensees.berkeley.edu>.
[4] Fathieh A, Mercan O. Three-dimensional, nonlinear, dynamic analysis of modular steel buildings. Struct Congress 2014;2014:2466–77.
[5] Filiatrault A, Tremblay R, Christopoulos C, Folz B, Pettinga D. Elements of structural dynamics and earthquake engineering. 3rd ed. Presses Internationals Polytechnique; 2013.
[6] National Building Code of Canada, NBCC 2010. Institute for Research in Construction, National Research Council of Canada, Ottawa, Ontario, Canada.
[7] Annan CD, Youssef MA, El Naggar MH. Experimental evaluation of the seismic performance of modular steel-braced frames. Eng Struct 2009;31(7):1435–46.
[8] Lawson RM, Richards J. Modular design for high-rise buildings. Proc Inst Civ Eng Struct Build 2010;163(SB3):151–64.
[9] Lawson RM, Ogden RG, Bergin R. Application of modular construction in high-rise buildings. American Society of Civil Engineers; 2012. pp. 148–154.
[10] Scott MH, Fenves GL. Plastic hinge integration methods for force-based beam–column elements. J Struct Eng 2006;132(2):244–52.
[11] Uriz P, Mahin SA. Seismic vulnerability assessment of concentrically braced steel frames. Int J Steel Struct 2004;4(4):239–48.
[12] Vamvatsikos D, Cornell CA. Investigating the influence of elastic spectral shape on the limit-state capacities of a 9-story building through IDA. In: 13th World conference on earthquake engineering. Paper No. 1463. Vancouver, BC, Canada, August 1–6, 2004.
[13] Vamvatsikos D, Cornell CA. The incremental dynamic analysis and its application to performance-based earthquake engineering. In: 12th European conference on earthquake engineering paper reference 479, 2002.
[14] Han SW, Chopra AK. Approximate incremental dynamic analysis using the modal pushover analysis procedure. Earthquake Eng Struct Dynam 2006;35(15):1853–73.
[15] FEMA 356. Prestandard and Commentary for the Seismic Rehabilitation of Buildings. Federal Emergency Management Agency, Washington, DC; 2000.